Biochimica et Biophysica Acta, 647 (1981) 95–111
Elsevier/North-Holland Biomedical Press

BBA 79366

MELITTIN BOUND TO DODECYLPHOSPHOCHOLINE MICELLES

^{1}H-NMR ASSIGNMENTS AND GLOBAL CONFORMATIONAL FEATURES

LARRY R. BROWN and KURT WÜTHRICH

Institut für Molekularbiologie und Biophysik, Eidgenössische Technische Hochschule, ETH-Hönggerberg, CH-8093 Zürich (Switzerland)

(Received March 18th, 1981)

Key words: Melittin; ^{1}H-NMR; Protein-lipid interaction; Dodecylphosphocholine micelle

Assignments have been obtained for most of the ^{1}H-NMR lines of melittin bound to fully deuterated dodecylphosphocholine micelles by combined use of two-dimensional spin echo correlated spectroscopy and one-dimensional NMR methods. Nuclear Overhauser enhancement measurements showed that the mobility of the entire polypeptide chain is reduced by binding of melittin to the detergent micelle and that the amino-terminal and carboxy-terminal halves of the primary structure constitute separate, compact domains within the conformation of micelle-bound melittin. p^{2}H titration experiments showed that the presence of positive charges on the four amino groups of melittin had little influence on the conformation of the micelle-bound polypeptide. Titration of tetrameric melittin with detergent provided evidence that melittin assumes similar conformations as a self-aggregated tetramer and as a monomer bound to micelles.

Introduction

Melittin is a polypeptide of 26 amino acids which constitutes about 50% of the dry weight of bee venom. At sufficiently high concentrations, melittin directly leads to lysis of native or model lipid membranes [1–5]. At low concentrations melittin leads to membrane lysis by activation of either the phospholipase A_2 found in bee venom [5–8] or of endogenous phospholipase found in *E. coli* membranes [6] and in a variety of types of cultured mammalian cells [9]. Low concentrations of melittin have also been found to affect membrane functions such as mitochondrial respiration [3], adenylate cyclase activity [10,11] and coupling in photosynthetic membranes [12]. It has recently been suggested that melittin is an example of a class of toxocological agents which subvert normal phospholipid turnover, thereby inducing a prolonged hydrolysis of phospholipids which eventually leads to dissolution of cell membranes [9].

Since the available evidence suggests that melittin exerts its physiological effects through interaction with membrane lipids, we have been interested in determining the structural basis of the melittin-lipid interactions. In previous studies, we have used high resolution ^{1}H-NMR and various physico-chemical methods to characterize conformational features of melittin in three different states, i.e. monomeric melittin in aqueous solution [13], tetrameric melittin in aqueous solution [14] and monomeric melittin bound to lipids [15,16]. These studies indicated that although monomeric melittin in aqueous solution has a flexible, extended conformation [13], melittin assumed better defined conformations either upon

Abbreviation: SECSY, spin echo correlated spectroscopy (two-dimensional).

self-aggregation to form a tetramer or upon binding to various types of detergents or phospholipids [14–16]. These studies also indicated that interaction of melittin with detergents and phospholipids might be regarded as 'mixed micelle formation', i.e. a lipid-water interface provided by micelles or bilayers appeared to be necessary to bind melittin to lipids, but both the type of lipid aggregate, i.e. micelles or bilayers, and the chemical nature of the interface were found to have little influence on the conformation of lipid-bound melittin [15].

Since melittin forms a stoichiometrically well defined complex with dodecylphosphocholine, i.e. mixed micelles containing one polypeptide and approx. 40 detergent molecules [15], and since a high resolution ^{1}H-NMR spectrum suitable for detailed analysis is obtained for melittin bound to fully deuterated micelles [16], we have used ^{1}H-NMR to further define the conformation of melittin bound to deuterated dodecylphosphocholine micelles. This paper describes the identification of numerous proton resonances in micelle-bound melittin and a characterization of global static and dynamic features of the conformation of micelle-bound melittin. The resonance assignments presented here provided a basis for further studies of more detailed structural properties of distinct segments of the melittin amino acid sequence and for investigations of the location of micelle-bound melittin relative to the micellar surface [17] (to be published).

Materials and Methods

The synthesis of fully deuterated dodecylphosphocholine [16] and the purification of melittin [13] have been described previously. All experiments were performed with the purified major component of *Apis mellifera* melittin, i.e. the minor component which is formylated at the α-amino group of Gly-1 had been removed. Previously described methods [18] were used for preparation of samples for NMR measurements. The composition of these samples is described in the figure captions.

^{1}H-NMR spectra at 360 MHz were recorded on a Bruker HX 360 spectrometer. Spin-decoupling difference spectra [19], truncated driven nuclear overhauser enhancement difference spectra [20,21] and two-dimensional spin-echo correlated spectra [22] were recorded as previously described. In some cases the resolution of the ^{1}H-NMR spectra was improved by multiplying the free induction decays with a phase-shifted sine bell [23,24]. Chemical shifts are given in parts per million (ppm) relative to an internal reference of sodium 3-trimethylsilyl[2,2,3,3-$^2H_4$]-propionate in aqueous solution at p^{2}H 7.0 [25]. Values given for p^{2}H are pH-meter readings uncorrected for isotope effects. Ionization constants, pK_a, were determined by non-linear least-squares fits of the experimental chemical shifts at varying pH values to one-proton titration curves.

Results

In the first part the experiments used to identify most of the ^{1}H-NMR resonances of melittin bound to deuterated dodecylphosphocholine micelles are described. The second part describes investigations in which the resonance assignments have been used to study global conformational features of micelle-bound melittin.

Assignment of the ^{1}H-NMR resonances of melittin bound to deuterated dodecylphosphocholine micelles

Although there are only 26 amino acid residues, assignment of the ^{1}H-NMR resonances of micelle-bound melittin was complicated by the amino acid composition of this polypeptide [27]

Gly-Ile-Gly-Ala-Val-Leu-Lys-Val-Leu-Thr-Thr-Gly-Leu-Pro-
1 5 10

-Ala-Leu-Ile-Ser-Trp-Ile-Lys-Arg-Lys-Arg-Gln-Gln-NH_2 .
15 20 25

Thus, while proline, serine and tryptophan are present only once in melittin, there are four leucine residues and three residues each of glycine, lysine and isoleucine. Consequently, assignment of the ^{1}H-NMR resonances of micelle-bound melittin involved problems which are normally encountered only for considerably larger polypeptide chains and use of a variety of different NMR experiments was necessary. These included two-dimensional spin echo correlated spectroscopy (SECSY) [22,28,29], 'null point difference decoupling' (see below), nuclear Overhauser enhancement difference spectroscopy [20,26], decoupling in nuclear Overhauser enhancement difference spectra [20], detergent titration and p^{2}H

titration. In addition to the resonance assignments, these experiments also provided considerable information on structural and dynamic features of micelle-bound melittin, consideration of which is deferred to the Discussion. Table I shows the resonance assignments which have been obtained for melittin bound to deuterated dodecylphosphocholine micelles.

Evidence for assignment of many of the resonance of micelle-bound melittin was obtained from a two-dimensional spin echo correlated spectrum of $8 \cdot 10^{-3}$ M melittin in the presence of 0.36 M [$^2H_{38}$]-dodecylphosphocholine at p^{2}H 5.5 and 55°C. Fig. 1 shows the 0–5 ppm spectral region of the SECSY spectrum. In this spectrum, if protons which give rise to resonances at chemical shifts δ_A and δ_B in one-dimensional NMR spectra have a scalar coupling, then with $\delta_A < \delta_B$ and $\Delta\delta = \delta_B - \delta_A$, cross peaks will be observed at the positions (δ_A, $-\Delta\delta/2$) and (δ_B, $\Delta\delta/2$) in the two-dimensional SECSY spectrum, i.e.

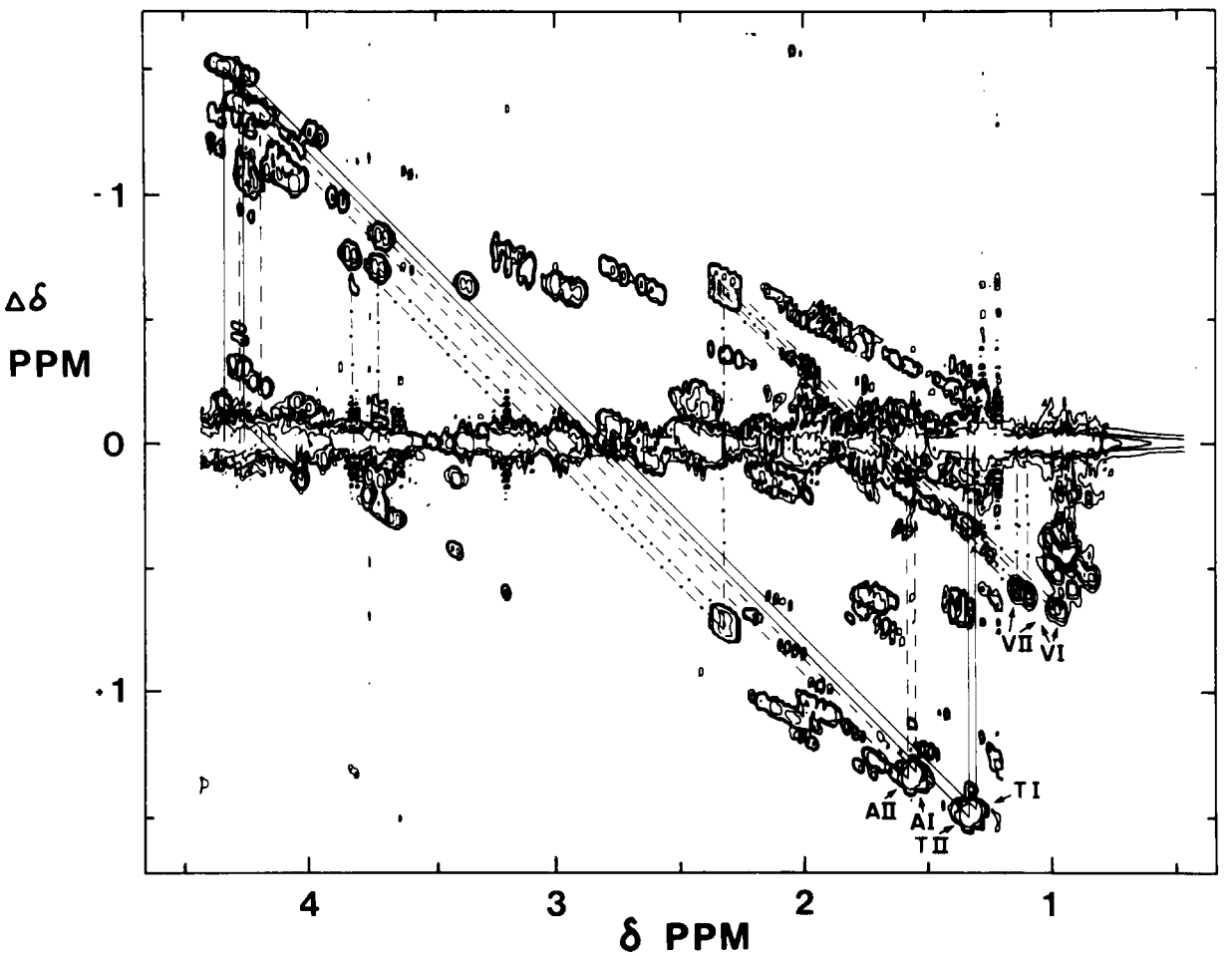

Fig. 1. Contour plot of the spectral region from 0.5 to 4.5 ppm of a 360 MHz spin echo correlated (SECSY) ^{1}H-NMR spectrum of melittin bound to deuterated dodecylphosphocholine micelles. The spectrum was recorded with a solution of $8 \cdot 10^{-3}$ M melittin and 0.36 M [$^2H_{38}$]dodecylphosphocholine in ^2H_2O at p^{2}H 5.5 and 55°C. Prior to this experiment the labile protons had been replaced with deuterium and the sample sealed under an N_2 atmosphere. The chemical shift, δ, on the horizontal axis corresponds to that in conventional, one-dimensional spectra. $\Delta\delta$ on the vertical axis stands for the difference frequencies between correlated nuclei. Cross peaks between J-coupled nuclei are at $\pm\Delta\delta/2$. Connectivities between the individual components of the following spin systems are indicated: ———, Thr-I and Thr-II (10 and 11); - - - - - -, Ala-I and Ala-II (4 and 15); – · – · –, Val-I and Val-II (5 and 8).

TABLE 1

RESONANCE ASSIGNMENTS FOR THE 360 MHz ^{1}H-NMR SPECTRUM OF MELITTIN BOUND TO DODECYLPHOSPHOCHOLINE MICELLES

Measured for $8 \cdot 10^{-3}$ M melittin and 0.36 M [$^2H_{38}$]dodecylphosphocholine at p^{2}H 5.5 and 37°C [a].

Residue [b]	Chemical shifts (ppm)			Coupling constants (Hz)	
	αCH	βCH	Others	$^3J_{\alpha\beta}$	J_{other}
Gly-1	4.04 3.94				$J_{\alpha\alpha}$, 15.4
Gly-I (3 or 12)	4.032 3.738				$J_{\alpha\alpha}$, 16.2
Gly-II (3 or 12)	4.205 3.748				$J_{\alpha\alpha}$, 16.6
Ala-I (4 or 15)	4.195	1.561			
Ala-II (4 or 15)	4.291	1.593			
Thr-I (10 or 11)	4.031	4.284	γCH_3, 1.331		
Thr-II (10 or 11)	4.025	4.352	γCH_3, 1.351	3.0	
Val-I (5 or 8)	3.706	2.33	γCH_3 1.108, 0.980	9.8	
Val-II (5 or 8)	3.824	2.33	γCH_3 1.160, 1.004	8.8	
Ile-2 [c]	4.024	1.97	γCH_3 1.023 { γCH 1.33, 1.63 δCH_3 0.980 }	5.4	
Ile-I (17 or 20) [c]	3.692	2.07	γCH_3 0.998 { γCH 1.25, 1.75 δCH_3 0.897 }	10.6	
Ile-II (17 or 20) [c]	3.327	2.12	γCH_3 0.921 γCH 1.27, 2.24 δCH_3 0.947	7.5	
Ser-18	4.206	4.04 4.09			
Trp-19	4.254	3.40 3.72	ring C2H 7.372 C4H 7.560 C5H 6.851 C6H 7.028 C7H 7.490	10.1	$J_{\beta\beta}$, 13.6
Lys-I (7, 21 or 23)	3.927	1.45 1.45	γCH 0.60 0.90 δCH_2 1.35 ϵCH 2.560, 2.742		$J_{\gamma\gamma}$, 12.4 $J_{\epsilon\epsilon}$, 12.3
Lys-II (7, 21 or 23) [d]			δCH_2 1.75 ϵCH_2 2.93		
Lys-III (7, 21 or 23) [d]	4.147	2.00 2.00	δCH_2 1.75 ϵCH_2 2.978		
Leu-I (6, 9, 13 or 16) [d]	4.264	1.70 1.70	γCH 1.95 δCH_3 0.857, 0.893		
Leu-II (6, 9, 13 or 16) [d]	4.380	2.00 1.75	γCH 1.89 δCH_3 0.910 0.970		
Leu-III (6, 9, 13 or 16) [d]			γCH 1.78 δCH_3 1.041, 0.937		
Leu-IV (6, 9, 13 or 16) [d]	3.862	1.95 1.95	γCH 1.87 δCH_3 1.016, 0.965		
Pro-14 [d]	4.268	2.43 2.14			
Arg-I (22 or 24)	4.087	1.94 1.80	γCH 1.60, 1.80 δCH_2 3.22		
Arg-II (22 or 24)	4.076	1.96 1.80	γCH 1.68, 1.78 δCH_2 3.114		
Gln-I and II (25 and 26) [c]	4.19	2.05 2.15	γCH_2 2.43		

[a] The SECSY spectrum was run at 55°C, all the other experiments at 37°C. The only residues for which appreciable changes in chemical shift between 37 and 55°C were detected were Ile-II and Lys-I. Both of these residues are spatially near to the indole ring of Trp-19 (Figs. 9, 10) and the chemical shifts are therefore particularly sensitive to small conformational changes.

[b] Roman numerals are used for resonances which have not been individually assigned. They denote corresponding residues in the spectra of monomeric melittin (13) and of the tetrameric melittin (14). The numbers refer to positions in the amino acid sequence.

the cross peaks lie on a line which makes a 135° angle with the $\Delta\delta = 0$ axis [22,28,29]. As has been described previously [29], the different types of amino acid spin systems show patterns in SECSY spectra which, in favourable cases, allow the type of amino acid to be directly identified. For example, in Fig. 1 the connectivities are shown for the αCH and βCH_3 resonances of two alanines, the αCH, βCH and γCH_3 resonances of two threonines and the αCH, βCH and $\gamma_{1,2}CH_3$ resonances of two valines.

Melittin contains a total of 22 methyl groups from 2 alanines, 2 threonines, 2 valines, 3 isoleucines and 4 leucines. The region of the SECSY spectrum shown in Fig. 2 contains cross peaks corresponding to the 18 methyl groups of valine, leucine and isoleucine. Even though there are 16 methyl resonances which strongly overlap between 0.86 and 1.04 ppm in the one-dimensional spectrum, individual cross peaks corresponding to almost all of these methyl groups could be observed in the SECSY spectrum. The cross peaks for the δCH_3 resonances of two leucines, which were overlapped at $\delta = 0.97$, $\Delta\delta = -0.46$ (Fig. 2), were the only exception. However, because some of the βCH and γCH_2 resonances of isoleucine and the γCH resonances of leucine also had overlapping chemical shifts (Table I), unambiguous assignments from the SECSY spectrum alone could be obtained only for seven of the 14 methyl groups of the leucines and isoleucines. Assignments of the other seven methyls were further based on the one-dimensional null point difference decoupling experiments as described in the following.

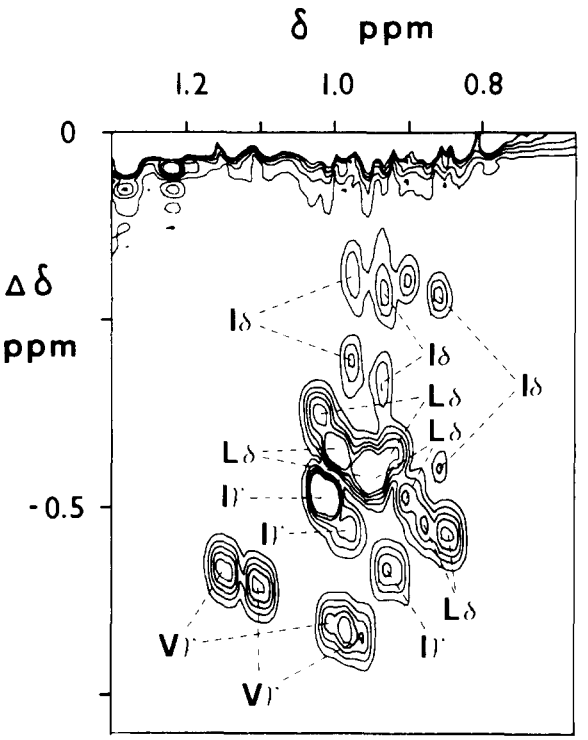

Fig. 2. Expanded plot of the region $\delta = 0.65$ to 1.30 ppm and $\Delta\delta = 0$ to −0.8 ppm in the SECSY spectrum of Fig. 1. This region contains cross peaks from the 18 methyl groups of the two valines, three isoleucines and four leucines of melittin. The assignments of the cross peaks are indicated by the one-letter code for the amino acid type and by a Greek letter for the position of the methyl group in the amino acid side chain. Note that there are two cross peaks for each δCH_3 of isoleucine, manifesting the connectivities with the two non-equivalent γ-methylene protons.

In order to detect decoupled multiplets in crowded one-dimensional ^{1}H-NMR spectra of proteins, it is usually necessary to use difference decoupling, i.e. to obtain the difference between spectra recorded with and without decoupling [19, 21]. Here, we have used a modification of the difference decoupling experiment, i.e. 'null point difference decoupling'. Difference spectra were obtained by subtracting a spectrum recorded with irradiation at frequency $\omega_B + n \cdot \Delta\omega$ from a spectrum recorded with irradiation at frequency $\omega_A + n \cdot \Delta\omega$, where both frequencies were in crowded spectral regions. A series of difference spectra were recorded for $n =$

[c] The γCH_2 and δCH_3 resonances of Ile-2 and Ile-I have not been assigned to the individual residues. The assignment of the Ile-II γCH_2 and δCH_3 resonances is based on the observations that in Overhauser effect measurements with short preirradiation times, the αCH, βCH and γCH at 2.24 ppm were found to be spatially close to one another and to the C4H of the indole ring of Trp-19.

[d] Resonances which must correspond to five αCH-βCH_2 fragments of two lysines, four leucines and Pro-14 were observed but not assigned to amino acid types.

[e] The resonances of glutamines 25 and 26 were overlapped. The chemical shifts for both residues are within ±0.02 ppm of the values given in the table.

0,1,2....., i.e. in each successive difference spectrum both decoupling frequencies were shifted by the same amount so that the difference between the two decoupling frequencies, $\omega_A - \omega_B$, was held constant. When $|\omega_A - \omega_B|$ is small, the appearance in the difference spectrum of spurious peaks from Bloch-Siegert effects [30], is minimized and when $\Delta\omega$ is small, the chemical shift of the irradiated resonance can be determined fairly accurately (see below). The actual values chosen for $\omega_A - \omega_B$ and $\Delta\omega$ depended on the purpose of the experiment. For example, we first screened the spectral region from 2.4 to 1.2 ppm using $\Delta\omega = \omega_A - \omega_B$ and $\omega_A - \omega_B = 0.1$ ppm, and then used smaller values of $\omega_A - \omega_B$ and $\Delta\omega < |\omega_A - \omega_B|$ to determine more accurate chemical shifts for the valines, leucines and isoleucines.

A series of null point difference decoupling experiments which were used to identify the αCH, βCH and γCH_3 resonances of one of the isoleucines is shown in Fig. 3. Fig. 3B shows that subtraction of a spectrum with $\omega_B = 2.12$ ppm from a spectrum with $\omega_A = 2.16$ ppm gives a difference spectrum in which a methyl doublet at 0.92 ppm is decoupled to a singlet, with the singlet showing a negative intensity. In the difference spectra shown in Fig. 3C and 3D, both decoupling frequencies have been shifted by $n \cdot \Delta\omega = -0.02$ and -0.04 ppm, respectively. In Fig. 3C, the intensity at 0.92 ppm is essentially nulled whereas in Fig. 3D the decoupled methyl singlet at 0.92 ppm shows a positive intensity. The spectra shown in Fig. 3 indicate that the methyl doublet at 0.92 ppm is more strongly decoupled at 2.12 ppm than at 2.16 ppm (Fig. 3B) or at 2.08 ppm (Fig. 3D), but is approximately equally decoupled at 2.14 and 2.10 ppm (Fig. 3C). From these experiments it is apparent that the methyl doublet at 0.92 ppm is coupled to a resonance at 2.12 ± 0.01 ppm. The observation in Fig. 3 that a single methyl doublet was decoupled by irradiation at 2.12 ppm indicates that this methyl doublet probably corresponds to an isoleucine γCH_3 group, i.e. the βCH resonance has been irradiated. The decoupling frequencies were in a crowded spectral region in these experiments (Fig. 3A) and a number of other resonances were also decoupled (Fig. 3B–3D). However, in the spectral region expected to contain the αCH resonances, i.e. 3.0–4.5 ppm, only the doublet resonance at 3.33 ppm shows the same dependence of the intensity on $n \cdot \Delta\omega$ as the decoupled methyl singlet at 0.92 ppm. Thus, the decoupled singlet resonance at 3.33 ppm is negative in Fig. 3B, nulled in Fig. 3C and positive in Fig. 3D. Resonances at 3.33, 2.12 and 0.92 ppm have there-

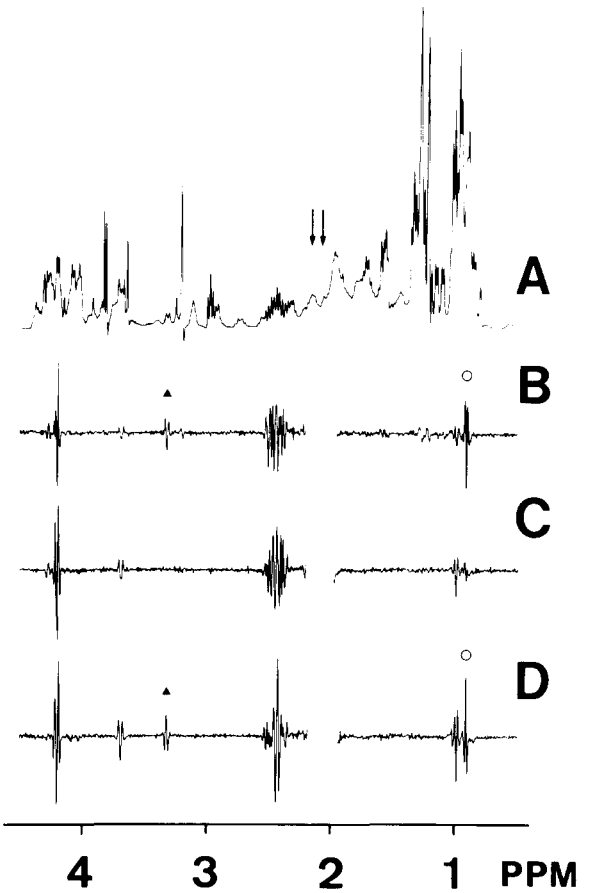

Fig. 3. Null point difference decoupling experiment used to assign the αCH (▲), βCH and γCH_3 (○) resonances of Ile-II (17 or 20). The same sample described in the caption to Fig. 1 was used at 37°C. (A) 0.5–4.5 ppm spectral region of the 360 MHz ^{1}H-NMR spectrum of melittin bound to deuterated dodecylphosphocholine micelles. (B) to (D) Spin-decoupling difference spectra [19] obtained by subtracting a free induction decay recorded with irradiation at δ_B from a free induction decay recorded with irradiation at δ_A. The chemical shifts corresponding to the irradiation frequencies were: (B) $\delta_A, \delta_B = 2.16, 2.12$ ppm; (C) $\delta_A, \delta_B = 2.14, 2.10$ ppm and (D) $\delta_A, \delta_B = 2.12, 2.08$ ppm. The arrows in (A) show chemical shifts of 2.16 and 2.08 ppm, i.e. they bound the region where double resonance irradiation was applied. In (B) to (D), the region near the irradiation frequencies has been omitted.

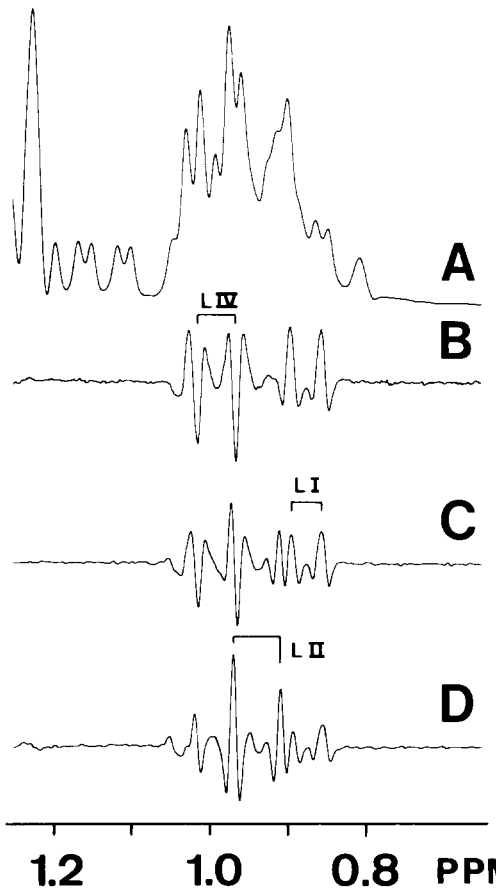

Fig. 4. Null point difference decoupling experiment used to assign the γCH and $\delta_{1,2}CH_3$ resonances of Leu-II and Leu-IV. The same sample described in the caption to Fig. 1 was used at 37°C. (A) 0.8–1.2 ppm spectral region of the 360 MHz ^{1}H-NMR spectrum of melittin bound to deuterated dodecylphosphocholine micelles. (B) to (D) Spin-decoupling difference spectra [19] obtained by subtracting a free induction decay recorded with irradiation at δ_B from a free induction decay recorded with irradiation at δ_A. The chemical shifts corresponding to the irradiation frequencies were: (B) δ_A, δ_B = 1.91, 1.87 ppm; (C) δ_A, δ_B = 1.90, 1.86 ppm; (D) δ_A, δ_B = 1.89, 1.85 ppm. The brackets in (B) and (D) denote the resonances assigned to the $\delta_{1,2}CH_3$ groups of Leu-IV and Leu-II, respectively. Decoupling of the $\delta_{1,2}CH_3$ resonances of Leu-I, for which γCH is at 1.95 ppm (Table I), was also apparent and the corresponding resonances are denoted by the bracket in (C).

fore been assigned to αCH, βCH and γCH_3, respectively, of an isoleucine.

Fig. 4 shows the experiments which were used to identify the γCH and $\delta_{1,2}CH_3$ resonances of leucines II and IV. These assignments were particularly demanding since one δCH_3 group from each of the two leucines had almost identical chemical shifts and since the γCH resonances of these two residues were separated by only 0.02 ppm (Table I). Because of the close similarity of the two γCH chemical shifts, a small value of $\Delta\omega = -0.01$ ppm was used in the experiments of Fig. 4. Two methyl doublets which decouple to singlets at 0.970 and 0.910 ppm have positive singlet intensities in Figs. 4C and 4D but are nulled when the irradiation frequencies are at 1.91 and 1.87 ppm (Fig. 4B). Resonances at 1.89, 0.970 and 0.910 ppm were therefore assigned to the γCH and $\delta_{1,2}CH_3$ groups, respectively, of Leu-II. Similarly, two methyl doublets which decouple to singlets at 1.016 and 0.965 ppm have negative singlet intensities in Figs. 4B and 4C but are essentially nulled when the two irradiation frequencies are at 1.89 and 1.85 (Fig. 4D). Resonances at 1.87, 1.016 and 0.965 ppm were therefore assigned to the γCH and $\delta_{1,2}CH_3$ groups, respectively, of Leu-IV (Table I). A useful feature of null point difference decoupling for these assignments was that by placing the two decoupling frequencies symmetrically to higher and lower field from a leucine γCH resonance, the methyl doublets which were decoupled by irradiation of this resonance could be nulled, thereby permitting unperturbed observation of other decoupled resonances. As mentioned earlier, the cross peaks of Leu-II and Leu-IV in the SECSY spectrum were partially overlapped at δ = 0.97, $\Delta\delta = -0.46$ (Fig. 2) so that the definite assignments could only be obtained by the experiments of Fig. 4. Similarly, all of the methyl resonances of micelle-bound melittin could be assigned to amino acid types.

In the SECSY spectrum of micelle-bound melittin (Fig. 1), a number of cross peaks were observed between resonances in the 3.5–4.5 ppm spectral region. An expansion of this region of the SECSY spectrum is shown in Fig. 5. From the amino acid composition of melittin, the region of the SECSY spectrum shown in Fig. 5 would be expected to contain resonances from the ABX spin systems of αCH and βCH_2 of Ser-18 and Trp-19, A_2, AB or AX spin systems from glycines 1, 3 and 12, the AM portion of the AMX_3 spin systems of threonines 10 and 11 and possibly resonances from δCH_2 of Pro-14. One ABX spin system with resonances at 3.40, 3.70 and 4.25

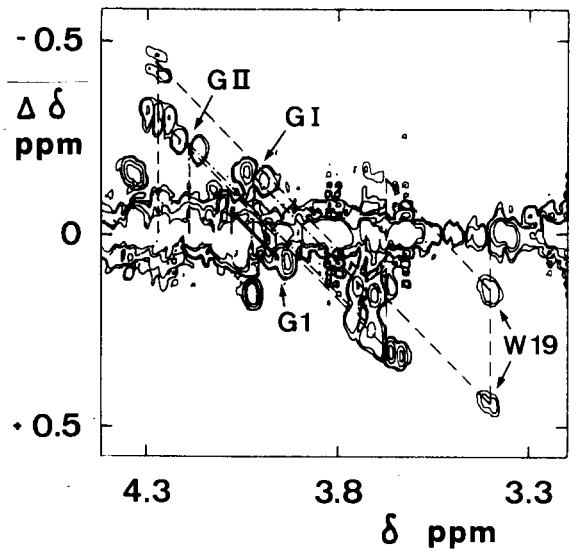

Fig. 5. Expanded plot of the region δ = 3.2 to 4.4 ppm and $\Delta\delta$ = −0.6 to +0.6 ppm in the SECSY spectrum of Fig. 1. The connectivities between the individual components of the following spin systems are shown: ------, αCH-βCH_2 of Trp-19; – · – · –, Gly-I and Gly-II (3 and 12); ———, Gly-1.

ppm is readily apparent in Fig. 5. Specific assignment of this spin system to Trp-19 is described below. As was demonstrated previously [29], SECSY spectra provide a powerful method for identifying glycine resonances in the crowded αCH region of protein ^{1}H-NMR spectra. Indeed, for micelle-bound melittin two AX spin systems with coupling constants $J > 15$ Hz, which is characteristic for glycine, were observed at 4.03 and 3.74 ppm, and at 4.21 and 3.75 ppm. Additional cross peaks at 4.04 and 3.94 ppm appeared to

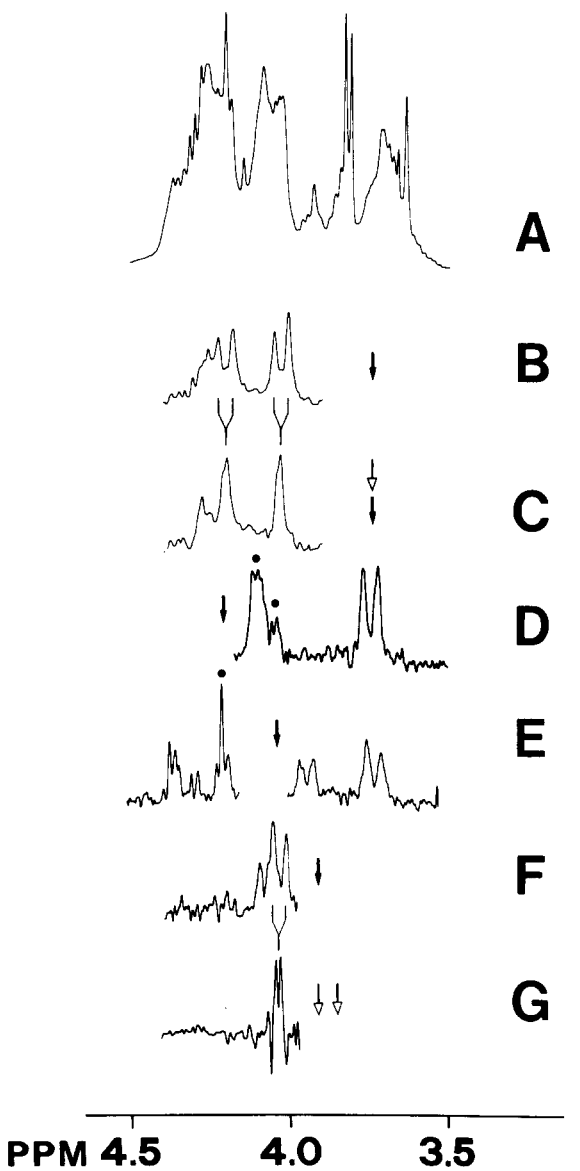

Fig. 6. 360 MHz ^{1}H-NMR experiments showing the AX spin systems of the three glycine residues in melittin. The same sample described in the caption to Fig. 1 was used at 37°C. The solid arrows denote the frequencies at which preirradiation for 0.4 s prior to data acquisition was used to build up nuclear Overhauser effects. The open arrows denote the frequencies used for decoupling during data acquisition. (A) 3.5–4.5 ppm spectral region of the ^{1}H-NMR spectrum of melittin bound to deuterated dodecylphosphocholine micelles. (B)–(F) Truncated driven nuclear Overhauser enhancement difference spectra obtained with preirradiation at: (B) 3.74 ppm, the αCH resonances of both Gly-I (3.74 ppm) and Gly-II (3.75 ppm) were preirradiated; (C) 3.74 ppm, with decoupling at 3.74 ppm, i.e. the αCH resonances of Gly-I and Gly-II were both preirradiated and decoupled; (D) 4.21 ppm, an αCH of Gly-II was preirradiated. (E) 4.04 ppm, the αCH resonances of both Gly-1 and Gly-I were preirradiated; (F) 3.92 ppm, an αCH resonance of Gly-1 was preirradiated. (G) The spin-decoupling difference spectrum [19] obtained by subtraction of a free induction decay recorded with decoupling at 3.87 ppm from a free induction decay recorded with decoupling at 3.92 ppm. The Gly-1 αCH resonance at 4.04 ppm is partially decoupled. To avoid non-selective irradiation of the Gly-2 αCH resonance at 4.04 ppm, the Gly-1 αCH resonance at 3.94 was preirradiated slightly off-resonance in (F) and decoupled slightly off-resonance in (G). In traces D and E resonances of Ser-18 are denoted by • (see text).

correspond to the third glycine (Fig. 5). These glycine assignments have also been obtained by nuclear Overhauser enhancement difference spectroscopy (Fig. 6). Preirradiation at 3.74 ppm led to observation of doublet resonances at 4.03 and 4.21 ppm (Fig. 6B) with coupling constants of 16.2 and 16.6 Hz, respectively. With preirradiation at 3.74 ppm and decoupling during acquisition at the same frequency, the doublets at 4.03 and 4.21 ppm were both decoupled to singlets (Fig. 6C). Similarly, preirradiation at 4.21 ppm gave a doublet at 3.75 ppm with a coupling constant of 16.6 Hz (Fig. 6D) and preirradiation of 4.04 ppm gave a doublet at 3.74 ppm with a coupling constant of 16.2 Hz (Fig. 6E). Fig. 6E contains a further doublet at 3.94 ppm with a coupling constant of 15.4 Hz. Preirradiation at this resonance position gave an Overhauser effect for a doublet at 4.04 ppm (Fig. 6F), which was assigned to a glycine AX spin system by the difference decoupling experiment of Fig. 6G.

Three resonances at 4.21, 4.09 and 4.04 ppm have been assigned to the αCH and βCH_2 hydrogens, respectively, of Ser-18, which is the only ABX spin system in melittin other than Trp-19. In Fig. 6D, preirradiation at 4.21 ppm gave Overhauser effects at 4.09 and 4.04 ppm. Furthermore, preirradiation at 4.04 ppm gave a strong triplet resonance at 4.21 ppm in the Overhauser effect difference spectrum (Fig. 6E) and difference decoupling experiments showed that a triplet resonance at 4.21 ppm was coupled to resonances at 4.09 and 4.04 ppm.

Identification of the resonances from the peripheral hydrogens of the side chains of lysine, arginine and glutamine as well as specific assignments for Gly-1, Ile-2 and Trp-19 were obtained by titration of tetrameric melittin with dodecylphosphocholine and by pH titration of micelle-bound melittin. Fig. 7 shows the changes in chemical shift observed for selected resonances of $4 \cdot 10^{-3}$ M melittin in 0.05 M phosphate buffer at p^2H 7.0 and 37°C as a function of the dodecylphosphocholine/melittin ratio. Under these conditions melittin forms a tetrameric aggregate in the absence of detergent [14] whereas a complex consisting of a single melittin molecule bound to a dodecylphosphocholine micelle is formed at high dodecylphosphocholine/melittin ratios [15]. The resonances shown in Fig. 7 could either be directly observed in the ^{1}H-NMR spectrum, or were identified at the various detergent ratios by difference decoupling experiments. Since continuous changes in chemical shift were observed as a function of the detergent/polypeptide ratio and since we have previously given resonance assignments for tetrameric melittin [14], corresponding resonances in the spectra of micelle-bound melittin could be identified from the titration curves in Fig. 7. Most importantly, the titration curves obtained for αCH and γCH_3 of Ile-2 and one βCH of Trp-19 (Fig. 7) allowed individual assignments of the resonances of these residues to be made in micelle-bound melittin (Table I).

For all the resonances shown in Fig. 7, the chemical shifts of micelle-bound melittin could also be measured over the entire p^2H range from p^2H 3.0 to p^2H 11.5. The vast majority of the resonances showed at most very slight changes in chemical shift. In this case, it is safe to assume that those resonances which showed major changes in chemical shifts as a function of p^2H must arise from hydrogen atoms which are near, in the covalent structure, to titratable groups. Fig. 8 shows the p^2H titration curves for all those resonances which showed changes in chemical shift $\geqslant$0.05 ppm between p^2H 3.0 and p^2H 11.5. Above p^2H 8.0, two doublet resonances from one of the three glycine residues titrated to chemical shift positions where they could be directly observed in the ^{1}H-NMR spectrum. When experiments of the type shown in Fig. 6 were repeated at p^2H 9.5, it was found that the resonances of only one of the three glycine residues showed large changes in chemical shift between p^2H 5.5 and p^2H 9.5. Since an upfield shift of approx. 0.5 ppm and an apparent pK_a of 7.7 (Fig. 8) were appropriate for titration of the α-amino group of an N-terminal glycine [31], the resonances at 3.94 and 4.04 ppm at p^2H 5.5 were assigned to Gly-1. In the same p^2H range, the αCH resonance assigned to Ile-2 shifted 0.1 ppm to higher field with an apparent pK_a of 7.7 (Fig. 8), whereas the chemical shifts of the other two isoleucine residues were virtually constant. Since the change in chemical shift and the apparent pK_a are typical for the second residue of a polypeptide chain [31], the p^2H titration data provided further evidence for the assignment of Ile-2. The only other resonances for which appreciable changes in chemical shift were detected between p^2H 7 and p^2H 9 were the αCH and βCH resonances of Val-I, which shifted 0.03 ppm to higher field, and

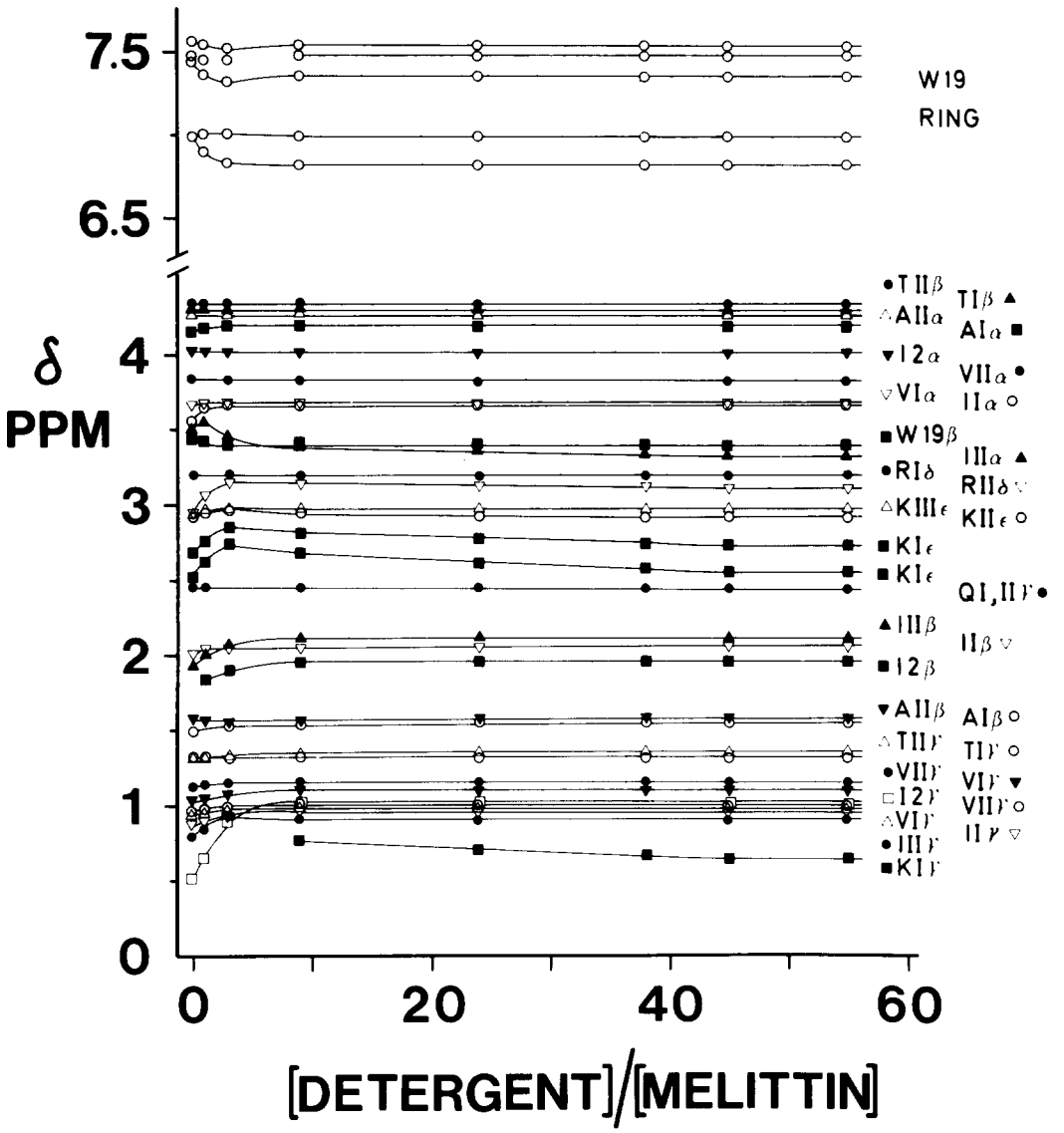

Fig. 7. For selected resonances of melittin (see text), plots are shown of the chemical shift observed as a function of the dodecylphosphocholine/melittin ratio. A $4 \cdot 10^{-3}$ M solution of melittin in 0.05 M phosphate buffer at p^2H 7.0 and 37°C was used. Under these conditions and in the absence of detergent, melittin is tetrameric [14]. For detergent/polypeptide ratios greater than approx. 40 : 1 [15], melittin is bound to the dodecylphosphocholine micelles as a monomer.

0.04 ppm to lower field, respectively. At higher p^2H, the ϵCH_2 resonances of Lys-II and Lys-III shifted 0.34 and 0.38 ppm to high field with apparent pK_a values of 10.0 and 10.1, respectively. For Lys-I, only part of the titration curves could be observed for the one-proton ϵCH resonances as well as for the one-proton γCH resonance near 0.6 ppm (see below). An apparent pK_a of 9.9 ± 0.1 was estimated from this data. The only other resonance for which an appreciable change in chemical shift was detected between p^2H 9.0 and p^2H 11.5 was the αCH of Ile-II, which shifted 0.04 ppm to lower field.

Identification of the resonances from the peripheral hydrogen atoms of the side chains of lysine,

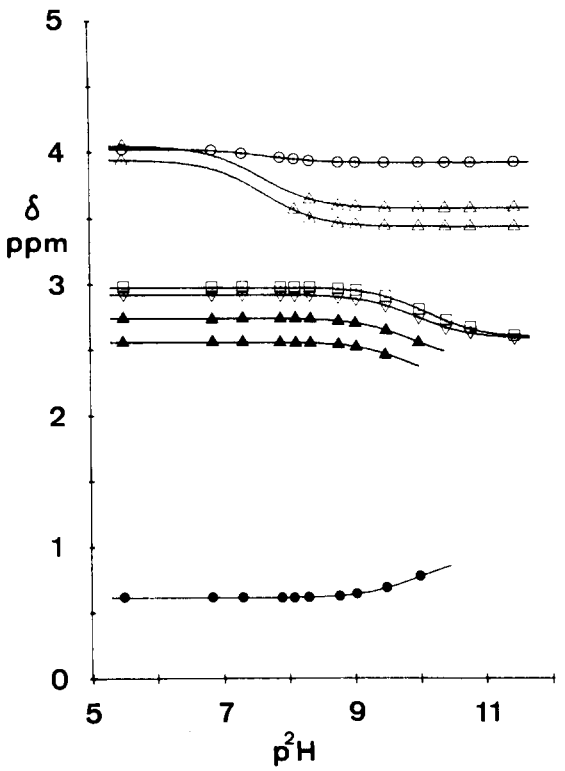

Fig. 8. For selected resonances of micelle-bound melittin, plots are shown of the chemical shift observed as a function of p^2H. Chemical shifts were obtained at the various p^2H values for all the resonances shown in Fig. 7, however, Fig. 8 includes only those resonances which showed changes in chemical shift of more than 0.05 ppm between p^2H 3.0 and p^2H 11.5. The solid curves were obtained by fitting the experimental points to one-proton titration curves. Titration curves are shown for: ○, αCH of Ile-2; △, αCH of Gly-1; □, ϵCH_2 of Lys-III (7, 21 or 23); △, ϵCH_2 of Lys-II (7, 21 or 23); ▲, two non-equivalent εCH's and ●, γCH of Lys-I (7, 21 or 23). (For the assignment of the γCH resonance of Lys-I, see Fig. 9).

arginine and glutamine from the detergent titration and p^2H titration experiments allowed further resonances of these residues to be identified from the SECSY spectrum. For the glutamine residues, the entire spin systems could be observed in the SECSY spectrum. These assignments were also obtained by difference decoupling and nuclear Overhauser effect difference experiments. The chemical shifts of the δCH_2 resonances of the lysines and the γCH_2 resonances of the arginines were identified from the SECSY spectrum. For Lys-I and the two arginines, the complete spin systems could then be identified.

Fig. 9 shows the experiments used to assign the resonances of Lys-I (Table I). In the ^1H-NMR spectrum of micelle-bound melittin, a high field one-proton resonance was observed at 0.60 ppm. Preirradiation of this resonance gave strong Overhauser effects at 0.90, 1.35 and 1.47 ppm and somewhat weaker Overhauser effects at an αCH triplet resonance at 3.93 ppm and at both εCH resonances of Lys-I at 2.74 and 2.56 ppm (Fig. 9B). Decoupling experiments showed that the one-proton resonance at 0.60 ppm was coupled to resonances at 0.90 ppm (Fig. 9D), 1.35 ppm (Fig. 9E) and 1.47 ppm (Fig. 9F). Furthermore, the αCH resonance at 3.93 ppm was decoupled by irradiation at 1.47 ppm (Fig. 9F) and the Lys-I εCH resonances at 2.74 and 2.56 ppm were decoupled at 1.35 ppm (Fig. 9E). From the SECSY experiment both βCH resonances were at 1.47 ppm and both δCH resonances of Lys-I at 1.35 ppm.

Similar experiments were used to assign the spin systems of the two arginines. For example, preirradiation of the Arg-I δCH_2 resonance at 3.12 ppm gave strong Overhauser effects for the γCH resonances at 1.78 and 1.68 ppm as well as for resonances at 1.96, 1.80 ppm and 4.08 ppm. Decoupling in nuclear Overhauser effect difference spectra then showed that the αCH resonance at 4.08 ppm was coupled to resonances at 1.96 and 1.80 ppm. Coupled resonances at these frequencies were also observed in the SECSY spectrum and in difference decoupling experiments. The resonance assignments for Arg-I shown in Table I were obtained from these experiments and analogous experiments were used to assign the resonances of Arg-II.

Global features of the conformation of micelle-bound melittin by nuclear Overhauser enhancement studies

For polypeptide chains bound to deuterated lipid micelles, highly selective ^1H-^1H Overhauser effects are obtained even with preirradiation times of several seconds [32,33]. As we have described in detail elsewhere [32,33], this characteristic of the Overhauser effects observed for micelle-bound polypeptide chains can be used to determine global structural features. This requires that a sufficient number of resonance assignments are available and that sizeable negative Overhauser effects are observed for most of the poly-

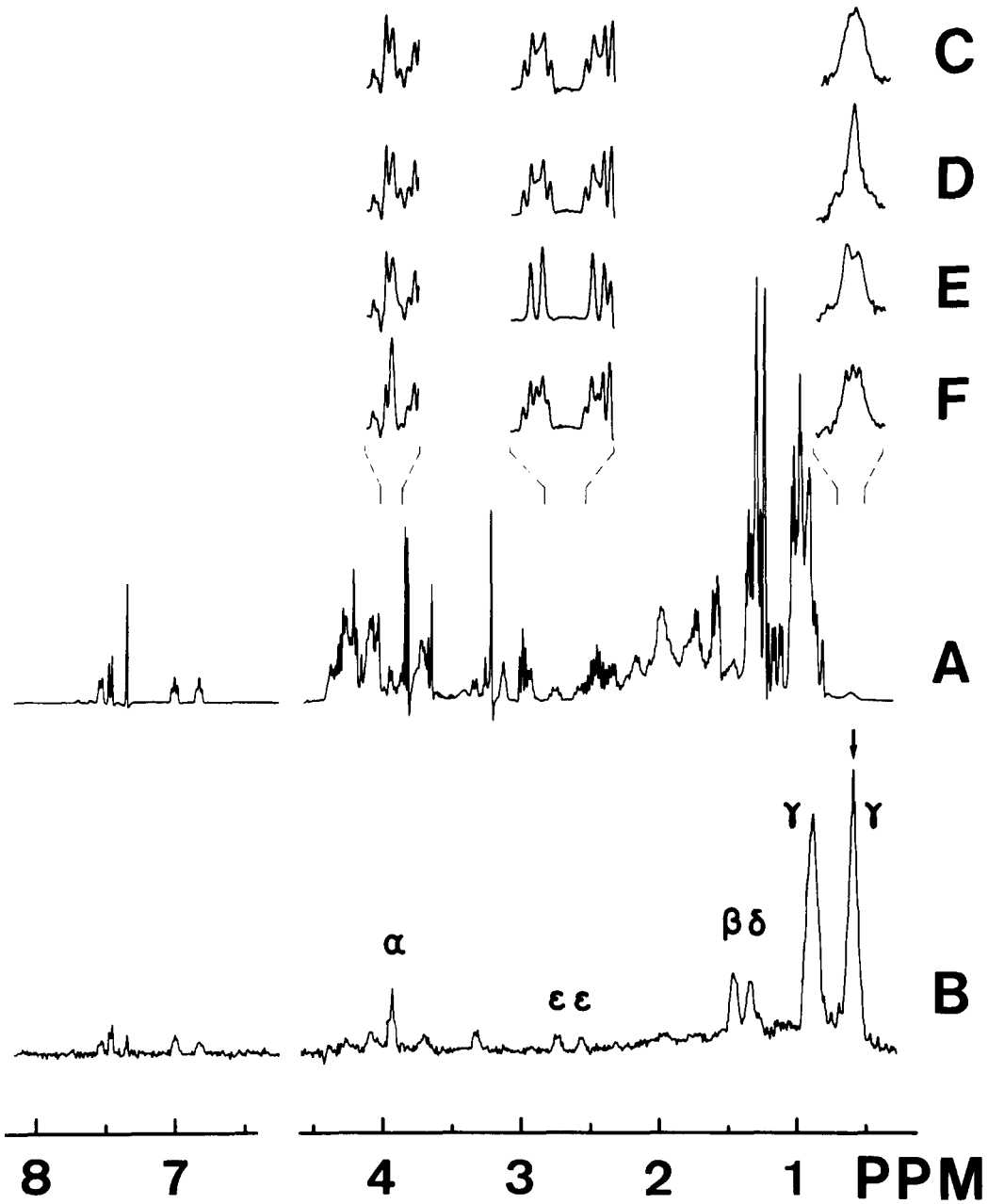

Fig. 9. Experiments used to assign the spin system of Lys-I. The same sample described in the caption to Fig. 1 was used at 37°C. (A) 360 MHz ^{1}H-NMR spectrum of melittin bound to deuterated dodecylphosphocholine micelles. (B) Truncated driven nuclear Overhauser enhancement difference spectrum obtained by preirradiation for 0.4 s of one of the Lys-I γCH resonances at 0.60 ppm arrow. Overhauser effects are observed for the following resonances of Lys-I: αCH, 3.93 ppm; βCH_2, 1.47 ppm; γCH, 0.90 ppm; δCH_2, 1.35 ppm and εCH, 2.56 ppm and 2.74 ppm. (C) to (F) Expanded plots of the spectral regions 0.50–0.70 ppm, 2.50–2.80 ppm and 3.88–3.98 ppm showing the effects of decoupling irradiation on selected resonances of Lys-I (note that in contrast to most other double irradiation experiments shown, these are not difference spectra). (C) No decoupling. (D) Decoupling irradiation at the γCH resonance at 0.90 ppm, the γCH resonance at 0.60 ppm is decoupled. (E) Decoupling irradiation at the δCH_2 resonance at 1.35 ppm, the γCH at 0.60 ppm and both εCH resonances at 2.56 and 2.74 ppm are decoupled. (F) Decoupling irradiation at the βCH_2 resonance at 1.47 ppm, the γCH resonance at 0.60 ppm and the αCH resonance at 3.93 ppm are decoupled.

peptide chain. In the case of micelle-bound melittin, extensive resonance assignments are now available. Furthermore, in the course of the experiments used to obtain the assignments in Table I and in additional Overhauser effect measurements (to be published), negative Overhauser effects have been observed for all the identified spin systems, i.e. for all residues except Pro-14.

Fig. 10 shows that with preirradiation times of 4 s, highly selective Overhauser effects are observed for melittin bound to deuterated dodecylphosphocholine micelles. For example, preirradiation of the C4H resonance of the indole ring of Trp-19 gave Overhauser effects at only a small proportion of the melittin resonances (Fig. 10B). Many of the resonances in Fig. 10B could be assigned directly from the observed chemical shifts, while other resonances have been assigned by decoupling in Overhauser enhancement difference spectra [20]. A majority of the resonances corresponded to Ile-II (17 or 20), Lys-I (7, 21 or 23), Leu-IV (6, 9, 13 or 16) and Trp-19. Many of the same resonances were observed when the indole C2H resonance was preirradiated (Fig. 10C). Of particular interest in this experiment was that weak Overhauser effects were observed at the δCH_2 resonances of both Arg-I and Arg-II (22 and 24) as well as for the ϵCH_2 resonances of Lys-I and Lys-II, i.e. two of the lysines 7, 21 and 23 (insert in Fig. 10C). A completely different set of resonances were observed in the Overhauser effect difference spectrum when the overlapping βCH resonances of Val-I and Val-II (5 and 8) were preirradiated for 4 s (Fig. 10D). In addition to the other resonances of the two valines, Overhauser effects were observed for methyl resonances of Ala-II (4 or 15), Thr-I (10 or 11), Leu-I and Leu-II (6, 9, 13 or 16) as well as for the αCH of Ile-2.

In evaluating the structural implications of these observations, it is important to note the distribution of amino acid residues in the melittin primary structure. The experiments shown in Figs. 10B and 10C show that presaturation of the C2H and C4H resonances from the indole ring of Trp-19 led to Overhauser effects at both of arginines 22 and 24 and for one of isoleucines 17 or 20, but that no Overhauser effects were detected for Ile-2, the valines (5 and 8), threonines (10 and 11) and glycines (1, 3 and 12), which are all located in the amino-terminal half of the amino acid sequence. Conversely, preirradiation of the βCH resonances of valines 5 and 8 (Fig. 10D) gave Overhauser effects for Ile-2 and one of threonines 10 and 11, but no Overhauser effects were detected for the resonances of Ser-18, Trp-19, isoleucines 17 and 20, arginines 22 and 24 or glutamines 25 and 26, all of which are located in the carboxy-terminal half of the amino acid sequence. Thus, the experiments in Fig. 10 indicate that Overhauser effects are observed amongst the group of residues located in the amino-terminal half of the primary structure and amongst the group of residues located in the carboxy-terminal half of the primary structure, but no Overhauser effects were detected between the two different groups of residues.

As has been discussed in detail elsewhere, when sizeable negative intra-residue Overhauser effects are observed for most of the polypeptide chain, then the detection of groups of residues which show intra-group but not inter-group Overhauser effects in measurements with long preirradiation times provides evidence for separate domains in the conformation of polypeptide chains bound to deuterated micelles [32, 33]. Thus, the amino-terminal and carboxy-terminal halves of the primary structure must constitute separate domains in the conformation adopted by melittin bound to dodecylphosphocholine micelles. Furthermore, although the alanines, lysines and leucines are located in both halves of the melittin amino acid sequence, the Overhauser effects observed for these residues would be consistent with separate domains for the amino-terminal and carboxy-terminal halves of micelle-bound melittin and suggest individual assignments for these residues. Thus, resonances from lysines I and II were associated with the carboxy-terminal group of residues (Fig. 10B and C) suggesting these lysines correspond to Lys-21 and Lys-23. Leu-IV was also associated with the carboxy-terminal group of residues (Fig. 10B and C) suggesting it corresponds to Leu-16, although Leu-13 cannot be entirely excluded. On the other hand, Ala-II and leucines I and II were associated with the N-terminal group of residues suggesting that these correspond to Ala-4 and leucines 6 and 9.

Discussion

The experiments described in this paper have allowed identification of a major proportion of the

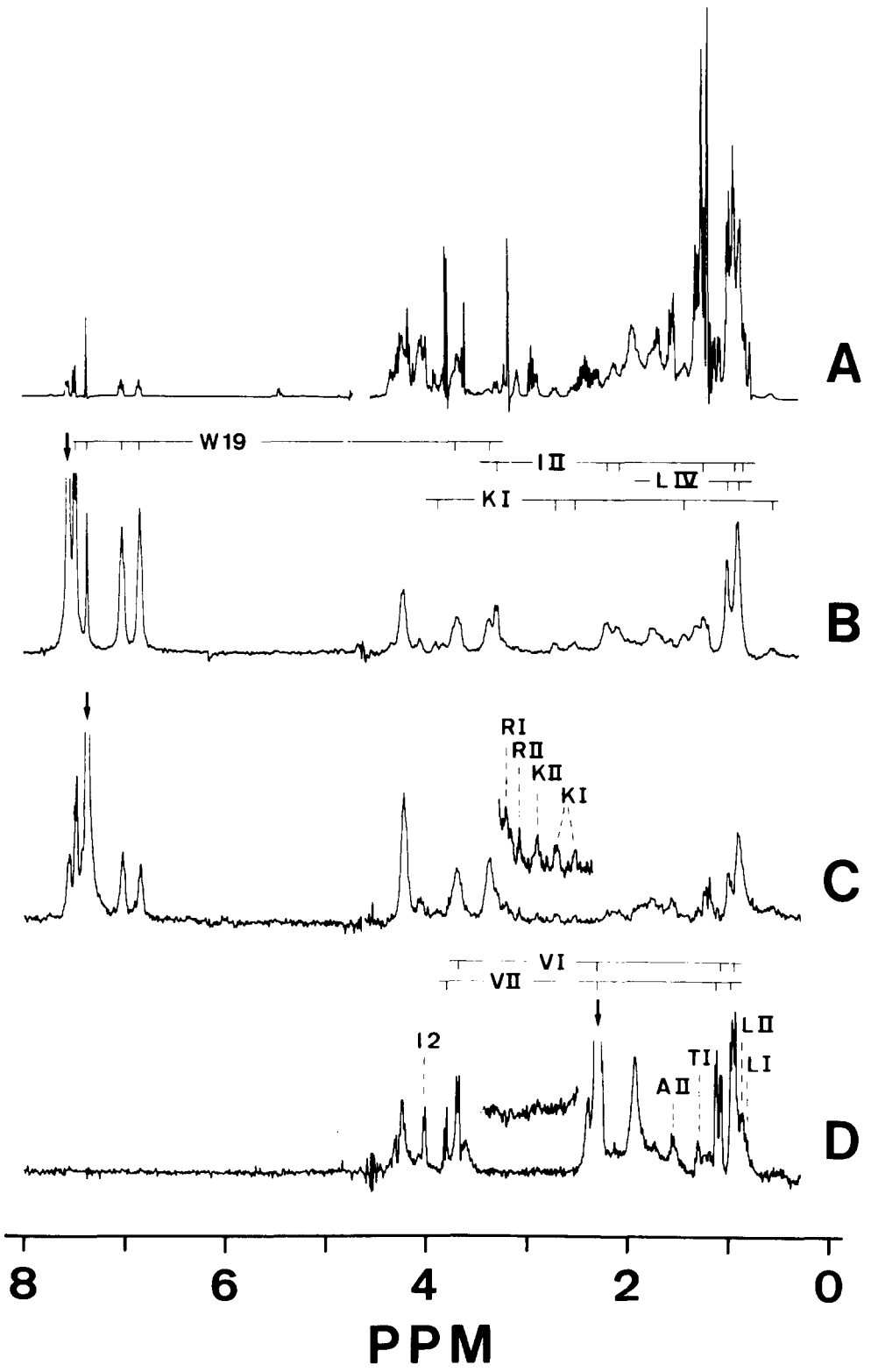
A
W19
I II
L IV
K I
B
RI
RII
KII
KI
C
VI
VII
I2
L II
L I
TI
A II
D
8
6
4
2
0
PPM

^{1}H-NMR lines of melittin bound to deuterated dodecylphosphocholine micelles. 96 resonances corresponding to 150 of the 179 non-labile hydrogen atoms in melittin have been assigned to amino acid types (Table I). This includes identification of the complete spin systems for 17 of the 26 amino acid residues and of all the resonances of Ile-2 and Ile-I (17 or 20). A further 12 resonances corresponding to 15 hydrogen atoms have been identified as corresponding to the αCH-βCH_2 fragments for five of the seven residues of lysine, leucine or proline (Table I). In view of the large number of assignments obtained, the experiments described in this paper provide a solid basis for investigation of structural features of micelle-bound melittin. In the following, consideration is given to the global structural and dynamic features of micelle-bound melittin revealed by the present experiments.

^{1}H-^{1}H Overhauser effect measurements provide a powerful method for detecting groups of hydrogen atoms which are separated by through-space distances of approx. 2.0 to 5.0 Å in molecular structures [21, 34,35]. They further manifest the rotational mobility of the observed molecular species, i.e. negative ^{1}H-^{1}H nuclear Overhauser enhancements are only observed when rotation relative to the external magnetic field of the vector joining the preirradiated and the observed hydrogen atoms is slow compared to the nuclear Larmor frequency, i.e. 360 MHz in the present experiments [34–36]. While positive ^{1}H-^{1}H Overhauser effects were observed for monomeric melittin in aqueous solution [16], sizeable negative nuclear Overhauser effects were observed for all the identified spin systems of melittin bound to dodecylphosphocholine micelles, i.e. for all residues except Pro-14. This indicates that for the entire amino acid sequence of melittin, binding of the polypeptide to the micelle results in reduced mobility; the rotational motions of individual segments of the polypeptide chain may even be restricted to rotation of the micellar complex as a whole. Independent of the ^{1}H-^{1}H Overhauser effects, the vicinal spin-spin coupling constants $^3J_{\alpha\beta}$ (Table I) provided additional, direct evidence for limited rotational mobility about the C^{α}-C^{β} bond [29,39] in individual amino acid residues, i.e. Thr-II (10 or 11), Val-I (5 or 8), Ile-2, Ile-I (17 or 20) and Trp-19. In globular proteins of the size of the melittin-dodecylphosphocholine complex, i.e. approx. 18 kdaltons [15], slow rotational motions lead to spin diffusion by cross relaxation within the closely packed spatial array of hydrogen atoms [36,37]. Thus, in nuclear Overhauser effect spectra recorded with preirradiation times of approx. 1 s or more, negative Overhauser effects can be observed for most of the hydrogen atoms in the protein [36–38]. In contrast, for micelle-bound melittin and for other polypeptide chains bound to deuterated micellar detergents [32,33], selective negative Overhauser effects were observed even with preirradiation times of several seconds. This indicates that the hydrogen atoms of micelle-bound melittin are not all included in a single, closely packed spatial array, i.e. micelle-bound melittin does not adopt a compact, globular structure.

Further structural information from the selective ^{1}H-^{1}H Overhauser effects in micelle-bound melittin can be obtained on the basis of the resonance assignments in Table I. Firstly, negative Overhauser effects between hydrogen atoms located in the same amino acid were observed throughout the molecule, showing that the individual amino acid residues were immobilized. Secondly, the absence of Overhauser effects between the two groups of resonances assigned to residues in the N-terminal segment 1–12 and in the C-terminal segment 16–26 shows that these two segments are separated by a distance of 5 Å or more

Fig. 10. ^{1}H-NMR experiments used to obtain information about the overall spatial structure of micelle-bound melittin (see text). The same sample described in the caption to Fig. 1 was used at 37°C. (A) 360 MHz ^{1}-H-NMR spectrum of melittin bound to deuterated dodecylphosphocholine micelles. (B) to (D): Truncated, driven nuclear Overhauser enhancement difference spectra obtained by preirradiation of selected resonances of micelle-bound melittin for 4 s prior to data acquisition. The preirradiated resonances (arrow) were: (B) C4H of the indole ring of Trp-19; (C) C2H of the indole ring of Trp-19; (D) βCH of Val-5 and Val-8. Assignments of the resonances for which Overhauser effects were observed are indicated by the one-letter code for the amino acid type and a number of Roman numeral for the spin system (Table I). For the spectral region containing the δCH_2 resonances of arginines 22 and 24 and the ϵCH_2 resonances of lysines 7, 21 and 23, the inserts in (C) and (D) show a 3-fold vertical expansion obtained after applying a 2-Hz line broadening to the free induction decay.

[18,32,33]. Finally, within both the amino-terminal region and the carboxy-terminal region, numerous negative interresidue Overhauser effects were observed (e.g. Fig. 10) indicating the two segments have relatively compact conformations. Overall this data therefore indicates that within the spatial structure of micelle-bound melittin, the N-terminal and C-terminal segments of the polypeptide chain form two compact, but spatially separated domains.

Although the Overhauser effect measurements indicated that the entire amino acid sequence of micelle-bound melittin is immobilized on a time scale of nanoseconds, two observations indicate that some portions of melittin may be further immobilized. Thus, the inequivalence in the ^{1}H-NMR spectrum of the two αCH resonances of Gly-1 and of the two ϵCH and two γCH resonances of Lys-I is a striking feature.

A possible explanation would be that for these residues rotation about the respective single bonds is slow on a millisecond time scale. It is attractive to consider that such immobilization might result from interaction of the respective positively charged amino groups with the phosphate groups of the dodecylphosphocholine molecules. However, the available evidence makes this an unlikely explanation. Firstly, the p^2H titration experiment (Fig. 8) indicated that the α-amino group of Gly-1 and the ϵ-amino groups of lysines 7, 21 and 23 all showed titration behaviour which was characteristic of an extended polypeptide in aqueous solution. Furthermore, the αCH resonances of Gly-1 and the ϵCH lines of Lys-I remained inequivalent when the respective amino groups were deprotonated (Fig. 8). That the non-equivalence of the Lys-I ϵCH resonances is not primarily due to interaction with lipid phosphate groups is further supported by the observations that these hydrogens also gave inequivalent resonances in the ^{1}H-NMR spectra obtained for tetrameric melittin in aqueous solution [14] and for melittin bound to non-ionic detergents [15]. It may also be noted that since most of the resonances of micelle-bound melittin showed virtually no change in chemical shift between p^2H 3.0 and p^2H 11.5, the presence of positive charges on the amino groups appears to have little or no influence on the conformation of micelle-bound melittin and not to be essential for binding of melittin to lipids.

In previous studies we have observed that tetrameric melittin and lipid-bound melittin gave similar circular dichroism spectra [15]. Although some differences in the ^{1}H-NMR spectra were observed between micelle-bound melittin and tetrameric melittin, only small variations of the chemical shifts were observed for melittin bound to various types of lipids or for tetrameric melittin under various solution conditions [14,15]. In contrast, markedly different CD spectra and ^{1}H chemical shifts prevailed for monomeric melittin in aqueous solution [13]. With the data in Table I, a more detailed comparison of tetrameric and micelle-bound melittin is now provided by the detergent titration curves shown in Fig. 7. For resonances from numerous residues distributed throughout the primary structure, most of the resonances of tetrameric melittin showed only slight changes in chemical shift upon going to micelle-bound melittin. Little or no change in chemical shift was observed for many of the side chain resonances and for all of the αCH resonances except those of Ile-I and Ile-II. Of those residues which showed the largest changes in chemical shift, i.e. Ile-2, Ile-II (17 or 20), Lys-I (7, 21 or 23) and Arg-II (22 or 24), all except Arg-II have been shown to experience appreciable ring current shifts from the indole ring of Trp-19 either in tetrameric [14] or micelle-bound melittin. The chemical shifts of these residues are therefore particularly sensitive to even small changes of conformation or of intermolecular contacts upon dissociation of the melittin tetramers. Overall, these observations indicate that for most hydrogen atoms in both tetrameric and micelle-bound melittin, the deviations of the chemical shifts from random coil values [39,40] are primarily determined by intramolecular interactions rather than intermolecular interactions with neighbouring melittin or lipid molecules, respectively. The spectral similarities then suggest that melittin adopts closely related conformations in the tetrameric form and when bound to micelles. The comparison of these two forms of melittin provides a particularly interesting illustration for the use of conformational studies of polypeptide chains in deuterated lipid systems [15–18,41].

The conclusions reached here thus indicate that structural explanation of the dynamic features as well as of the amphiphatic properties of the three-dimensional structure of melittin suggested by the modes of self-association or of interaction with lipids and detergents [14,15] will have to await detailed eluci-

dation of the conformations in the N-terminal and C-terminal domains. Work on micelle-bound melittin, using the resonance assignments of Table I and an extensive set of selective ^1H-^1H Overhauser effects as input for a distance-geometry algorithm [18], is currently in progress. In view of the apparent similarity of the molecular conformations for tetrameric and micelle-bound melittin, relevant structural data might also come from single crystal X-ray studies of aggregated melittin [42].

Acknowledgements

We would like to thank Dr. Anil Kumar for recording the SECSY spectrum. Financial support by the Swiss National Science Foundation (project 3.528.79) is gratefully acknowledged.

References

1 Habermann, E. (1972) Science 177, 314–322
2 Weissmann, G., Krakauer, K. and Hirschhorn, R. (1969) Biochem. Pharmacol. 18, 1771–1775
3 Olson, F.C., Munjal, D. and Malviya, A.N. (1974) Toxicon 12, 419–425
4 Hegner, D. (1969) Arch. Exp. Pathol. Pharmakol. 261, 118–132
5 Sessa, G., Freer, J.H., Colaccio, G. and Weissmann, G. (1969) J. Biol. Chem. 244, 3575–3582
6 Mollay, C., Kreil, G. and Berger, H. (1976) Biochim. Biophys. Acta 426, 317–324
7 Mollay, C. and Kreil, G. (1974) FEBS Lett. 46, 141–144
8 Yunes, R., Goldhammer, A.R., Garner, W.K. and Cordes, E.H. (1977) Arch. Biochem. Biophys. 183, 105–112
9 Shier, W.T. (1979) Proc. Natl. Acad. Sci. USA 76, 195–199
10 Lad, P.L. and Shier, W.T. (1980) Arch. Biochem. Biophys. 204, 418–424
11 Cook, G.H. and Wolff, J. (1977) Biochim. Biophys. Acta 498, 255–258
12 Berg, S.P., Davies, G.E. and Haller, A.M. (1980) FEBS Lett. 117, 143–148
13 Lauterwein, J., Brown, L.R. and Wüthrich, K. (1980) Biochim. Biophys. Acta 622, 219–230
14 Brown, L.R., Lauterwein, J. and Wüthrich, K. (1980) Biochim. Biophys. Acta 622, 231–244
15 Lauterwein, J., Bösch, C., Brown, L.R. and Wüthrich, K. (1979) Biochim. Biophys. Acta 556, 244–264
16 Brown, L.R. (1979) Biochim. Biophys. Acta 557, 135–148
17 Brown, L.R., Bösch, C. and Wüthrich, K. (1981) Biochim. Biophys. Acta 642, 296–312
18 Braun, W., Bösch, C., Brown, L.R., Gō, N. and Wüthrich, K. (1981) Biochim. Biophys. Acta 667, 377–396
19 De Marco, A., Tschesche, H., Wagner, G. and Wüthrich, K. (1977) Biophys. Struct. Mech. 3, 303–315
20 Richarz, R. and Wüthrich, K. (1978) J. Magn. Resonance 30, 147–150
21 Wagner, G. and Wüthrich, K. (1979) J. Magn. Resonance 33, 675–680
22 Nagayama, K., Kumar, A., Wüthrich, K. and Ernst, R.R. (1980) J. Magn. Resonance 40, 321–334
23 De Marco, A. and Wüthrich, K. (1976) J. Magn. Resonance 24, 201–204
24 Wagner, G., Wüthrich, K. and Tschesche, H. (1978) Eur. J. Biochem. 86, 67–76
25 De Marco, A. (1977) J. Magn. Resonance 26, 527–528
26 Gibbons, W.A., Crepeaux, D., Delayre, J., Dunand, J.J., Hadjukovic, G. and Wyssbrod, H.R. (1975) in Peptides: Chemistry, Structure and Biology (Walter, R. and Meienhofer, J., eds.), pp. 127–137, Ann Arbor Science
27 Habermann, E. and Jentsch, J. (1967) Hoppe-Seyler's Z. Physiol. Chem. 348, 37–50
28 Nagayama, K., Wüthrich, K. and Ernst, R.R. (1979) Biochem. Biophys. Res. Commun. 90, 305–311
29 Nagayama, K. and Wüthrich, K. (1981) Eur. J. Biochem., 114, 365–374
30 Bloch, F. and Siegert, A. (1940) Phys. Rev. 57, 522–527
31 Bundi, A. (1977) Ph.D. Thesis No. 6306, ETH Zürich
32 Wüthrich, K., Bösch, C. and Brown, L.R. (1980) Biochem. Biophys. Res. Commun. 95, 1504–1509
33 Bösch, C., Brown, L.R. and Wüthrich, K. (1980) Biochim. Biophys. Acta 603, 298–312
34 Noggle, J.H. and Schirmer, R.E. (1971) The Nuclear Overhauser Effect, Academic Press, New York
35 Bothner-By, A.A. (1979) in Biological Applications of Magnetic Resonance (Shulman, R.G., ed.), pp. 177–219, Academic Press, New York
36 Kalk, A. and Berendsen, H.J.C. (1976) J. Magn. Resonance 24, 343–366
37 Sykes, B.D., Hull, W.E. and Snyder, G.H. (1978) Biophys. J. 21, 137–146
38 Dubs, A., Wagner, G. and Wüthrich, K. (1979) Biochim. Biophys. Acta 577, 177–194
39 Wüthrich, K. (1976) NMR in Biological Research: Peptides and Proteins, North-Holland Publishing Company, Amsterdam
40 Bundi, A. and Wüthrich, K. (1979) Biopolymers 18, 285–297
41 Feigenson, G.W., Meers, P.R. and Kingsley, P.B. (1977) Biochim. Biophys. Acta 471, 487–491
42 Eisenberg, D., Terwillinger, T.C. and Tsui, F. (1980) Biophys. J. 32, 252–254